

---

# Harmony4D: A Video Dataset for In-The-Wild Close Human Interactions

---

Rawal Khirodkar\*, Jyun-Ting Song\*, Jinkun Cao, Zhengyi Luo, Kris Kitani  
Carnegie Mellon University

## Abstract

Understanding how humans interact with each other is key to building realistic multi-human virtual reality systems. This area remains relatively unexplored due to the lack of large-scale datasets. Recent datasets focusing on this issue mainly consist of activities captured entirely in controlled indoor environments with choreographed actions, significantly affecting their diversity. To address this, we introduce Harmony4D, a multi-view video dataset for human-human interaction featuring in-the-wild activities such as wrestling, dancing, MMA, and more. We use a flexible multi-view capture system to record these dynamic activities and provide annotations for human detection, tracking, 2D/3D pose estimation, and mesh recovery for closely interacting subjects. We propose a novel markerless algorithm to track 3D human poses in severe occlusion and close interaction to obtain our annotations with minimal manual intervention. Harmony4D consists of 1.66 million images and 3.32 million human instances from more than 20 synchronized cameras with 208 video sequences spanning diverse environments and 24 unique subjects. We rigorously evaluate existing state-of-the-art methods for mesh recovery and highlight their significant limitations in modeling close interaction scenarios. Additionally, we fine-tune a pre-trained HMR2.0 model on Harmony4D and demonstrate an improved performance of 54.8% PVE in scenes with severe occlusion and contact. Code and data are available at <https://jyuntins.github.io/harmony4d/>.

“*Harmony*—a cohesive alignment of human behaviors.”

## 1 Introduction

As social beings, humans frequently interact with each other using physical touch [73, 64, 35]. By studying these interactions, one can potentially unravel various aspects of human behavior, including emotions [24], intentions [13], and dynamics [59]. As with most problems in computer vision [36], a first step in modeling contact interactions involves building large-scale 3D multi-human datasets. Many such datasets [15, 74, 20, 80, 87, 57] have emerged in recent years. However, similar to most existing single-human datasets [28], contact interaction datasets lack subject and environment diversity and are captured under controlled indoor conditions with choreographed activities. Learning-based methods [42, 70, 43, 38] trained on such biased benchmarks struggle to generalize to real-world conditions. The core issue is that recovering high-quality ground-truth mesh for scenarios with frequent human-human contact is challenging due to severe occlusion, truncation, and dynamic movements [58]. Existing methods typically rely on extensive RGBD motion capture systems [80] or a large number of high-end wired camera systems (over 100) [31] to achieve accurate annotations. This reliance on extensive static capture systems makes in-the-wild data collection impractical [60]. Therefore, we ask: can we develop a markerless capture system that uses only a few cameras, is mobile, and is capable of accurately extracting 3D ground truth for in-the-wild scenarios involving contact interactions? To tackle this challenge, we introduce the *Harmony4D* dataset.

---

\*Equal contribution

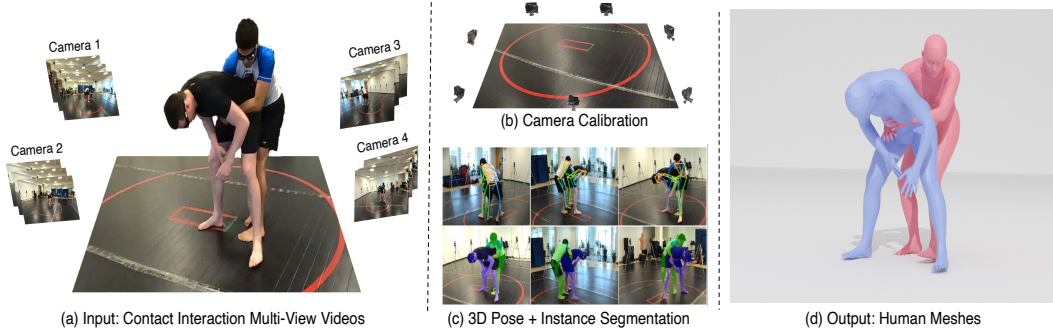


Figure 1: **Overview of Harmony4D setup.** (a) Multiple synchronized and calibrated cameras capture the contact interaction in *wrestling*. (b) We align all cameras into a gravity-aligned metric world coordinate system. (c) Our processing obtains per-view instance segmentation masks along with 3D keypoints. (d) Reconstructed ground-truth meshes after multi-step collision optimization.

Harmony4D is a novel dataset featuring high-resolution videos of dynamic activities with contact interactions such as wrestling, dancing, karate, MMA and fencing. In contrast to previous datasets, Harmony4D is collected in the wild with a specific focus on subject and environment diversity. Table 1 compares our dataset with existing 3D human datasets focusing on contact interactions. Harmony4D is a substantially large dataset, consisting of 1.66 million images captured from more than 20 synchronized cameras, resulting in 3.32 million visible human instances. Specifically, we provide comprehensive ground-truth annotations such as camera parameters, 2D bounding boxes [23], human tracking identities [86], 2D/3D human poses [68], and 3D human meshes [33]. Figure 1 provides an overview of the capture setup and annotation processing. The multi-camera setup is inspired by EgoHumans [39], utilizing Meta’s Aria glasses [54], which feature an RGB and two greyscale cameras for the subject’s first-person view, along with stationary RGB cameras for the third-person view. This combination allows us to accurately track and triangulate poses in 3D for extended periods without using visual markers [85] or additional sensors [1]. To our knowledge, Harmony4D is the only in-the-wild video dataset with dynamic activities and contact interactions.

Our annotation procedure minimizes the need for manual supervision. We divide any input multi-view video sequence into two stages: (i) pre-contact and (ii) post-contact. The pre-contact stage refers to the time interval before the first physical interaction between the subjects. We utilize an existing pose extraction algorithm [39] to obtain 3D poses during the pre-contact stage. However, existing methods face significant challenges in post-contact scenarios, primarily due to severe occlusion, truncation, and joint ambiguity when subjects are in very close proximity (e.g., during wrestling or dancing). For the challenging post-contact stage, we propose a novel algorithm that uses instance segmentation [40], segmentation-conditioned 2D pose estimation [51], and 3D pose forecasting [2] in a temporal feedback loop to accurately track 3D poses. Our key idea is to use segmentation-conditioned 2D pose estimation, see (c) in Figure 1, to reason about missing or completely hidden body parts and disambiguate between multiple human joints. Finally, we build an efficient multi-stage motion capture pipeline to fit the SMPL [52] body model to the 3D human skeletons, incorporating optimization to minimize mesh interpenetration.

Dataset	In-The-Wild	Scenes	Subjects	Cameras	Images	Instances	Mesh
ShakeFive2 [74]	✗	1	6	1	34K	68K	✗
MuPoTs-3D [57]	✗	3	8	8	8K	22K	✗
MultiHuman [87]	✗	1	8	6	32K	69K	✓
ExPI [20]	✗	1	4	68	1.9M	3.8M	✗
CHI3D [15]	✗	1	10	4	315K	728K	✓
Hi4D [80]	✗	1	40	8	88K	176K	✓
<b>Harmony4D (Ours)</b>	✓	5	24	20	1.66M	3.32M	✓

Table 1: **Comparison with existing 3D datasets with multi-human interactions.** *Subjects* and *Scenes* are number of unique subjects and capture environments. *Cameras* are number of stationary views per sequence. *Images* are number of images. *Instances* are number of visible human instances.



Figure 2: **Dataset Composition.** Harmony4D consists of diverse, dynamic activities such as dancing, karate, MMA, and wrestling, all captured in in-the-wild settings.

The extensive scale and diverse scenarios of the Harmony4D dataset enable a thorough evaluation and improvement of methods for human-human contact estimation. We specifically evaluate current techniques for human mesh regression, uncovering that existing methods often struggle with missing meshes, inaccurate pose predictions in the presence of occlusion, and handling the complexities of natural, unconstrained human interactions. Importantly, when we fine-tune off-the-shelf methods on our large training set, the fine-tuned methods generalize well to challenging contact interactions and even outperform specifically designed methods for human contact reasoning [58]. Moreover, we observe significant improvements in vertex contact prediction and occlusion reasoning. This underscores the need for Harmony4D, a large-scale dataset and a robust evaluation benchmark for in-the-wild contact interactions. The limitation is not necessarily with the methods [42, 70, 48, 46], but with the need to expose these methods to more extensive data in these underrepresented scenarios.

Our contributions are summarized as follows.

- A novel method based on multi-view instance segmentation and 3D human pose forecasting to extract 4D meshes of closely interacting humans.
- Harmony4D, a large-scale in-the-wild dataset with millions of multi-view images, parametric body models and vertex-level contact for dynamic and unchoreographed activities.
- Evaluation of existing state-of-the-art methods for monocular mesh regression, emphasizing their fundamental limitations in handling contact interactions, and demonstrating significantly improved performance when fine-tuned on our dataset.

## 2 Related Work

**Limited 3D Mesh Recovery Datasets.** Current progress in human vision research has been significantly driven by datasets [11, 76, 51, 28, 10, 16, 25, 45, 84]. However, unlike 2D pose datasets, 3D human mesh estimation datasets [28, 75, 56, 31, 32, 67, 79] are limited in diversity which significantly hampers the ability of deep models to generalize to the real world [82]. Popular 3D datasets like Human3.6M [28], AMASS [55], HumanEva [67], AIST++ [47], HUMBI [81], PROX [22], and TotalCapture [32] only contain single human sequences. Multi-human datasets like PanopticStudio [31],

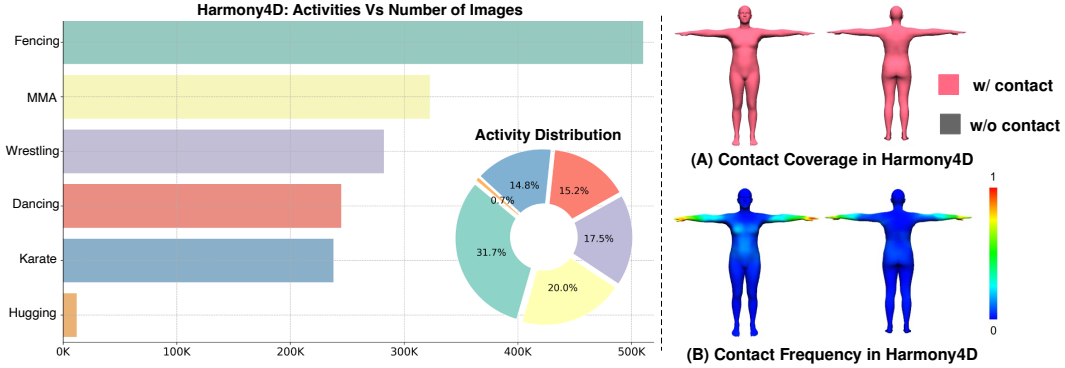


Figure 3: **Data Distribution.** The dynamic activities in the Harmony4D dataset cover all area for the SMPL body model. We visualize the most frequent body parts in contact during interactions as a normalized heatmap.

MuCo-3DHP [57], TUM Shelf [8] are limited to indoor lab conditions. Outdoor multi-human datasets like 3DPW [75], MuPoTS [57], and EgoHumans [39] do not focus on human-human interactions. The Harmony4D dataset goes beyond existing 3D mesh datasets in meaningful ways, capturing in-the-wild activities with frequent multi-human contact and a particular focus on subject and scene diversity, as well as unchoreographed activities.

**Human Pose and Shape Estimation.** Most approaches [49, 42, 50, 46, 19, 12, 83, 33, 9, 38, 69] rely on the SMPL model [52], which provides a low-dimensional parametrization of the human body. HMR [34] employs a neural network to regress the parameters of an SMPL body model from a single image. Follow-up works like 4DHumans [18], Multi-HMR [3], WHAM [66], BEV [70], ROMP [69], and PARE [42] have improved the robustness of the original method by using more annotations, larger models, and auxiliary conditioning information such as camera parameters, segmentation masks, and 2D poses. However, most methods require “full-body” single human images [62], limiting their robustness in scenarios where multiple humans are interacting due to the limited representation in the training data. Recent works like BUDDI [58] build a diffusion model on top of BEV [70]’s output as initialization to model the distribution of humans in proximity. Despite these advancements, we show that existing methods fail in scenarios with interacting humans in the Harmony4D dataset.

**Close Human Interaction Datasets.** Several contact-related datasets focus on human interactions with objects or static scenes [72, 4, 14, 22, 27, 71]. Additionally, recent datasets model close interactions between dynamic humans [80, 15, 74, 26, 31, 57, 20, 87]. ShakeFive2 [74] and MuPoTS-3D [57] only provide 3D keypoints and lack mesh or body shape information. CHI3D [15] uses an indoor motion capture system to fit parametric human models of at most one actor at a time. MultiHuman [87] provides textured scans of interacting people but lacks ground-truth level body model registrations. ExPI [20] contains dynamic textured meshes in addition to 3D joint locations but misses body model registrations and contact information. Furthermore, ExPI [20] includes only two pairs of dance actors. The most related dataset to ours is Hi4D [80], which uses a multi-view RGBD capture system to capture the 4D volume of two subjects interacting with each other. Hi4D uses online tracking and optimization to extract per person scans from the joint scans and fit a parametric body model to them. However, Hi4D is limited to a single indoor capture location and lacks background diversity, consisting of choreographed activities. In contrast, Harmony4D is collected in in-the-wild settings with unchoreographed dynamic activities.

### 3 Harmony4D

This section describes the data collection setup and our proposed in-contact human mesh tracking system. Our objective is to develop a markerless annotation pipeline that accurately provides ground truth 3D human shapes and poses from videos, even in cases of severe occlusions and multiple human contacts, with minimal manual intervention. The proposed capture and mesh tracking system builds upon EgoHumans [39] and extends to work effectively under post-contact conditions, including significant occlusions and truncations.

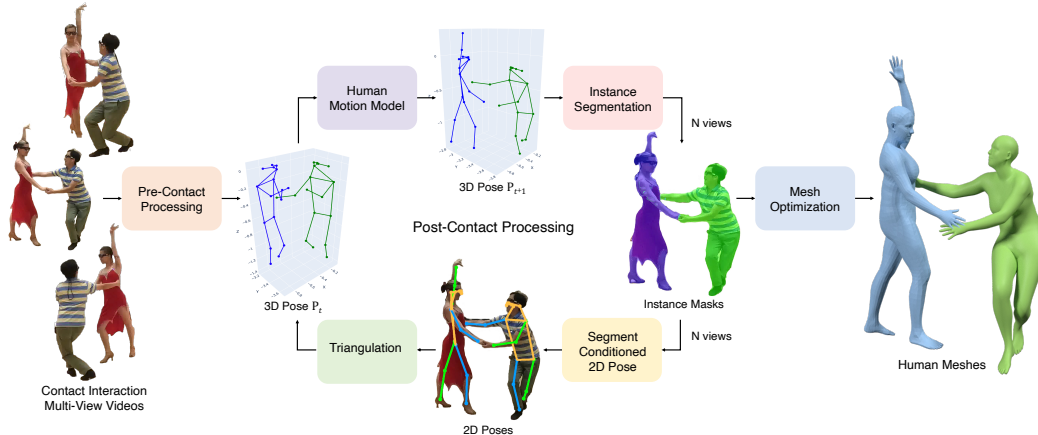


Figure 4: **Overview of Harmony4D processing setup.** Given a multi-view RGB video sequence, we divide it into pre-contact and post-contact stages. We estimate per-subject 3D poses in the pre-contact stage [39] as initialization. The post-contact stage uses sequential processing involving 3D pose forecasting with a human motion model, per-view 2D point-conditioned instance segmentation, and mask-conditioned 2D pose estimation, followed by multi-view triangulation and mesh fitting.

**Data Collection.** We aim to capture dynamic activities with human-human contact under in-the-wild conditions such as wrestling, dancing, fencing, etc. Figure 2 and Figure 3 show the captured dynamic activities and depicts the data distributions of activities in the Harmony4D dataset. In comparison to previous datasets, our sequences are not restricted to indoor conditions and consist of realistic contact interactions with over 1.6 million images. Following EgoHumans [39], to obtain high-quality ground truth, our capture setup includes multiple views using 20 GoPro cameras, refer Figure 1 (b). The video resolution is set to 4K ( $3840 \times 2160$ ) and recorded at a rate of 60 frames per second (FPS). Importantly, the volume created by our cameras is portable and can be moved across locations. All cameras are synchronized to ensure temporal consistency across different views. Optionally, we also include Aria glasses [54] to provide the egocentric perspective of subjects. Each sequence consists of two subjects. All participants were briefed on the research project, provided informed consent following IRB guidelines, and received monetary compensation for their participation.

**Camera Calibration.** We determine the intrinsic and extrinsic parameters for all cameras using structure from motion (SfM) [65] for each sequence. The world coordinate system is scaled to be metric and gravity-aligned. To ensure the registration of all cameras in a single coordinate system using SfM, we pre-scan the environment externally with an additional camera. For contact sequences with Aria glasses [54], we also transform the camera coordinates of the ego-glasses into the stationary camera coordinate system using Procrustes alignment [53].

**Pre-Contact Processing.** We divide a multi-view video sequence into two parts: (i) pre-contact, the time interval before the first subject-to-subject contact, and (ii) post-contact, the period after the first contact. We leverage the multi-person 3D pose estimation method from EgoHumans [39] to obtain 3D poses in the pre-contact stage. Our pre-contact processing is efficient, parallelizing all time-steps, and works accurately since the subjects are completely visible from most camera views during this stage.

### 3.1 Post-Contact Processing.

The main challenges in post-contact are detecting partially or completely occluded keypoints, associating these keypoints with the correct human identities, and ensuring that the estimated 3D human meshes remain spatially and temporally coherent while being consistent with the multi-view video evidence. To address this, we propose a novel sequential algorithm that leverages 3D human-pose forecasting, 2D point-conditioned instance segmentation, and mask-conditioned 2D pose estimation. Figure 4 provides an overview of Harmony4D post-contact processing.

**Human Motion Model.** To reason about occluded keypoints, we use 3D human pose forecasting with a human motion model based on Kalman filter (KF) [44]. KF is a linear estimator for dynamical systems discretized in the time domain which only requires the state estimations on a history of time

steps to estimate the next time step target state. Specifically, we train a per-subject 3D motion model in a sliding window fashion over a history of  $T$  frames to predict the future 3D keypoint locations. The forecasting model is initialized using the pre-contact poses. Assuming  $J$  keypoints, we use  $J$  filters to model the 3D motion of each keypoint independently. Each KF’s state  $\mathbf{x}$  is defined as  $\mathbf{x} = [x, y, z, \dot{x}, \dot{y}, \dot{z}]^\top$ , where  $(x, y, z)$  are the 3D keypoint coordinates and  $(\dot{x}, \dot{y}, \dot{z})$  are the velocities.

**Instance Segmentation.** We aim to infer the actual 3D keypoint locations at time step  $t + 1$  from the forecasted ones, accounting for discrepancies due to sudden motions like tackling or jumping. Most current methods rely on per-view 2D pose estimation using a bounding box and then multi-view triangulation [29]. However, bounding boxes are ambiguous [37] when subjects are close together, as seen in Figure 5 (Left). An off-the-shelf 2D pose estimator, given the subject bounding-boxes is unable to disentangle the subject poses accurately. Our key idea is to use instance segmentation masks as conditioning to a 2D pose estimator. We project the forecasted 3D poses to all views and apply the Segment-Anything model [40] using the target subject’s 2D pose as positive points and others’ poses as negative points. Our high frame rate processing ensures the forecasted 3D poses are close to the true ones, enabling reliable instance mask estimation across all views.

**Segmentation Conditioned 2D Pose Estimation.** We propose SegPose2D, a deep model for conditional 2D pose estimation, which takes both the RGB image patch and the binary segmentation mask as input to predict the 2D pose. SegPose2D uses the ViTPose [78] backbone with two transformer branches and feature fusion at multiple depths of the network. We train SegPose2D on the COCO [51] dataset using ground-truth segmentation masks. Figure 5 (Right) compares the mask-conditioned 2D pose estimation of SegPose2D with ViTPose [78] on a hugging sequence. The input mask is crucial for disentangling occluded human poses.

**Multi-View Triangulation.** Our triangulation setup follows the pre-contact processing [39]. Let  $C$  represent all synchronized video streams with known projection matrices  $P_c$ . We aim at estimating the global 3D pose  $\mathbf{y}_{j,t} \in \mathbb{R}^3$  of a fixed set of human keypoints indexed by  $j \in (1..J)$  at timestamp  $t \in (1..T)$  for all humans in the scene (omitting the human index for simplicity). Let  $\mathbf{x}_{c,j,t} \in \mathbb{R}^2$  be the  $j$ th 2D keypoint at time  $t$  from camera  $c$ . To infer 3D poses from 2D estimates, we use a linear algebraic multi-view triangulation approach [21]. Traditional triangulation assumes equal contribution from all 2D keypoints  $\mathbf{x}_{c,j,t}$ , but some views may be unreliable due to occlusions or framing issues, degrading the results. We apply RANSAC to address this. For each time step  $t$ , we solve:  $\tilde{\mathbf{y}}_{j,t}, A_{j,t}\tilde{\mathbf{y}}_{j,t} = 0$ , where  $A_{j,t} \in \mathbb{R}^{2C' \times 4}$  consists of components from the projection matrices and  $\mathbf{x}_{c,j,t}$  and  $C'$  is the cardinality of the camera inlier set post-RANSAC. Finally, we refine the 3D poses for the entire sequence using temporal smoothing, joint symmetry and bone constraints [7, 39].

**Mesh Optimization.** Given the 3D pose estimates  $\mathbf{y}_{\{1..T\}}$  for all subjects in a video sequence, we fit a human mesh to these 3D pose sequences to obtain the in-contact vertex annotations. The human mesh is represented using body pose and shape parameters,  $\boldsymbol{\theta} = [\boldsymbol{\theta}_{\text{pose}}, \boldsymbol{\theta}_{\text{shape}}, \boldsymbol{\theta}_{\text{global}}]$ , where  $\boldsymbol{\theta}_{\text{pose}} \in \mathbb{R}^{23 \times 6}$ ,  $\boldsymbol{\theta}_{\text{shape}} \in \mathbb{R}^{10}$ ,  $\boldsymbol{\theta}_{\text{global}} \in \mathbb{R}^6$ . The pose parameters  $\boldsymbol{\theta}_{\text{pose}}$  are the 6D representation of the joint rotations [88] of the 23 body joints of the SMPL [52] body. The shape parameters  $\boldsymbol{\theta}_{\text{shape}}$  are the first 10 coefficients of the PCA shape space derived from CAESAR [63] scans.  $\boldsymbol{\theta}_{\text{global}}$  consists of the global root orientation and translation of the body. Let  $\Phi : \boldsymbol{\theta} \rightarrow \mathbf{y}$  be a differentiable mapping function that projects SMPL parameters  $\boldsymbol{\theta}$  to corresponding 3D keypoints  $\mathbf{y}$ . Similar to EgoHumans [39], we fit  $\boldsymbol{\theta}$  to the 3D pose trajectory by minimizing  $\mathcal{L}_{\text{mesh}}$  defined as follows,

$$\begin{aligned} \mathcal{L}_{\text{mesh}}(\boldsymbol{\theta}) = & w_1 \|\mathbf{y} - \Phi(\boldsymbol{\theta})\|_2 + w_2 \|\boldsymbol{\theta}_{\text{pose}}\|_2 + w_3 \mathcal{L}_{\text{limb}}(\Phi(\boldsymbol{\theta})) + w_4 \mathcal{L}_{\text{symm}}(\Phi(\boldsymbol{\theta})) \\ & + w_5 \mathcal{L}_{\text{temporal}}(\Phi(\boldsymbol{\theta})) + w_6 \mathcal{L}_{\beta}(\boldsymbol{\theta}_{\text{shape}}) + w_7 \mathcal{L}_{\text{collision}}(\boldsymbol{\theta}) \quad (1) \end{aligned}$$

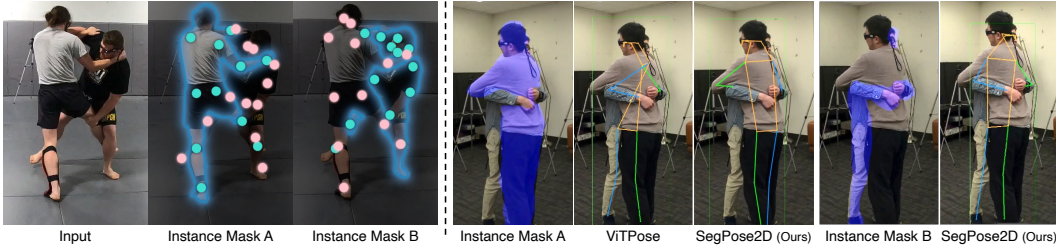


Figure 5: (Left) Point conditioned instance segmentation. Projected 3D keypoints as positive or negative prompts. (Right) Comparison of ViTPose [78] with mask-conditioned 2D pose estimation.

where  $\mathcal{L}_{\text{limb}}$  is the constant limb length loss,  $\mathcal{L}_{\text{symm}}$  is the body symmetry loss,  $\mathcal{L}_{\text{temporal}}$  is temporal smoothing,  $\mathcal{L}_{\beta}$  is the Gaussian mixture shape prior loss [6],  $\|\theta_{\text{pose}}\|_2$  penalizes hyper-extensions of joints,  $\mathcal{L}_{\text{collision}}$ , inspired by Interdiff [77], prevents mesh self and interpenetration and  $w_1..w_7$  are scalar weights. Compared to optimization in EgoHumans [39] where each subject mesh is fitted independently, the addition of the  $\mathcal{L}_{\text{collision}}$  is a crucial improvement for modeling in-the-wild multi-human contact scenarios. We define  $\mathcal{L}_{\text{collision}}(\theta) = \sum_{i=1}^N \sum_{j=1}^V \phi_i(x_j, y_j, z_j)$ , where  $N$  is the number of subjects, and  $V$  is the number of mesh vertices.  $\phi$  computes the negative penetration depth by  $\phi(x, y, z) = -\min(\text{SDF}(x, y, z), 0)$  where  $\text{SDF}(x, y, z)$  is the signed-distance field [30] at a vertex location  $(x, y, z)$ . This formulation ensures that the loss is positive when vertices penetrate themselves or other human meshes, thereby encouraging the separation of two human meshes as shown in Figure 6.

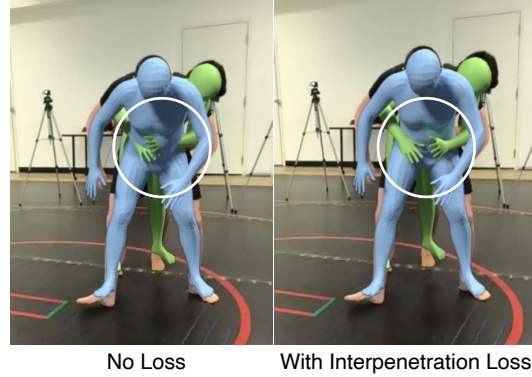


Figure 6: Mesh optimization with interpenetration loss.

## 4 Experiments

In this section, we first describe the evaluation of mesh recovery methods on our dataset. Then, we showcase ablative experiments that highlight the quality of the annotations provided by the dataset.

### 4.1 Implementation Details

We divide each sequence into shorter clips of at least 5 seconds at 20 FPS. The annotation per time step includes camera parameters, bounding boxes, person IDs, 2D/3D human poses, and 3D meshes per subject. All 3D poses at each time step are manually inspected and rectified in case of errors before performing mesh fitting. After mesh optimization, we manually verify and re-optimize each mesh sequence and contact vertices with custom hyperparameters if necessary. The number of keypoints  $J$  is set to 17 [51]. The human motion model uses history of 10 frames. We use the Segment-Anything-H [40] backbone for instance segmentation. SegPose2D is based of the ViTPose-H [78] backbone and is trained on 6 A100 GPUs for 5 days on the COCO [51] dataset. We use CLIFF [48] to obtain initial SMPL estimates for mesh optimization. To compute the SDF for mesh interpenetration loss, we use a custom GPU implementation by Jiang et al. [30] along with Geman-McClure [17] error for robustness. Figure 8 provides a multi-view visualization of the ground-truth mesh during contact interaction. We visualize the vertices in contact in Figure 7. For more visualization, please refer to the supplemental.

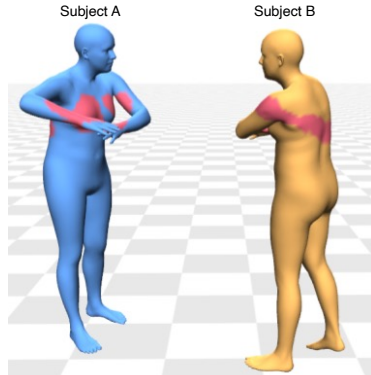


Figure 7: Ground-truth contact vertices for *hugging* sequence.

### 4.2 Benchmarking Mesh Recovery Methods

We evaluate existing state-of-the-art monocular mesh prediction methods such as PARE[41], HMR2.0[18], ROMP[69], BEV[70], Multi-HMR[3] and BUDDI[58] on the Harmony4D test set. For fairness, we use ground-truth bounding boxes as input to the top-down methods.

**Metrics.** We report standard metrics [75] such as MPJPE and PVE for mean joint and vertex errors, along with PA-MPJPE, PA-PVE, N-MPJPE, and N-PVE for their Procrustes-alignment and F1 score normalized variants, respectively. Additionally, we also report other metrics like 3DPCK, AUC [60]. To measure interpenetration during multi-contact, we compute maximum point-to-surface distance (mP2S) in mm. Note, for BUDDI and Multi-HMR, which predict SMPL-X [61] parameters instead of SMPL, we follow BEDLAM [5] and convert predicted SMPL-X meshes to SMPL using a fixed vertex mapping  $\mathcal{M} \in \mathbb{R}^{10475 \times 6890}$ .



Figure 8: Harmony4D ground-truth mesh visualized from six camera views for the *hugging* sequence.

**Discussion.** In contrast to a general dataset like 3DPW [75], we observe that the MPJPE for baseline methods is much higher on the challenging Harmony4D *test* set. For instance, off-the-shelf Multi-HMR [3] reports an MPJPE of 61.4 mm on 3DPW compared to 93.8 mm on the Harmony4D benchmark. Notably, Multi-HMR, a bottom-up method, performs significantly well compared to other baselines, even outperforming BUDDI [58], which is specifically trained and designed to model human-human contact. Among the top-down methods, HMR2.0 [18] performs the best with an MPJPE of 108.2 mm due to its large-scale training and the ViTPose [78] transformer backbone. Importantly, we also notice a very high normalized per vertex error (N-PVE) for all baselines, which is due to the failure in predicting a 3D consistent mesh in the presence of frequently occurring occlusions in our dataset. Harmony4D provides a unique and challenging evaluation benchmark for in-the-wild human contact interaction scenarios.

**Finetuning.** To demonstrate the utility of our dataset beyond serving as a challenging evaluation benchmark, we finetune HMR2.0 [18] on our *train* set. The Harmony4D *train* set is significantly larger than existing general datasets, containing more than 1.2 million images. We use a training setup similar to HMR2.0 [18] for finetuning. HMR2.0-finetuned demonstrates significant improvement across all metrics, see Table 2. It improves MPJPE by 55.9%, MPVPE by 54.8% and 3DPCK by 21.01%. Interestingly, we do not supervise HMR2.0 specifically with contact vertex annotations; however, we observe that the inter-contact relationships are preserved in the predictions. Figure 9 provides a qualitative comparison on the *test* set between BUDDI [58], HMR2.0 [18], and HMR2.0-finetuned alongside the ground truth annotations. The results show that our *train* set can serve as an effective source for adapting existing monocular mesh estimation methods to multi-human interaction settings.

### 4.3 Ablations

**Number of Cameras.** We investigate the impact of the number of cameras on the estimated 3D pose accuracy in our processing. Specifically, we uniformly sample 6 to 18 equidistant cameras from the camera perimeter and calculate the MPJPE between the resulting keypoints and our ground truth 3D keypoints obtained from all 20 cameras. Figure 10 shows the performance trend across various

Method	MPJPE ↓	PA-MPJPE ↓	N-MPJPE ↓	PVE ↓	PA-PVE ↓	N-PVE ↓	3DPCK ↑	AUC ↑	F1 ↑	mP2S ↓
PARE[41]	119.03	65.49	138.40	144.77	73.52	168.34	73.23	47.19	0.86	N/A
ROMP[69]	121.13	80.23	134.59	161.12	91.82	179.02	68.47	44.70	0.90	N/A
BEV[70]	111.29	78.04	119.66	144.28	90.13	155.14	74.63	48.94	0.93	134
BUDDI[58]	126.35	84.00	133.00	158.72	95.95	167.06	70.28	45.75	0.95	106
HMR2.0[18]	108.18	60.25	109.28	131.00	67.96	132.32	75.62	49.79	<u>0.99</u>	N/A
Multi-HMR[3]	<u>93.82</u>	<u>58.53</u>	<u>101.98</u>	<u>115.79</u>	<u>67.67</u>	<u>125.85</u>	<u>83.57</u>	<u>55.08</u>	0.92	53
<b>HMR2.0-finetune</b>	<b>47.71 (-46.11)</b>	<b>32.75</b>	<b>48.18</b>	<b>59.14</b>	<b>38.93</b>	<b>59.74</b>	<b>96.63</b>	<b>75.75</b>	<b>0.99</b>	N/A

Table 2: Comparison of monocular mesh recovery methods on the Harmony4D *test* set. mP2S metric is not reported for HMR2.0, PARE, and ROMP, as they predict each human instance in an independent coordinate system. Note, finetuning HMR2.0 improves performance significantly.

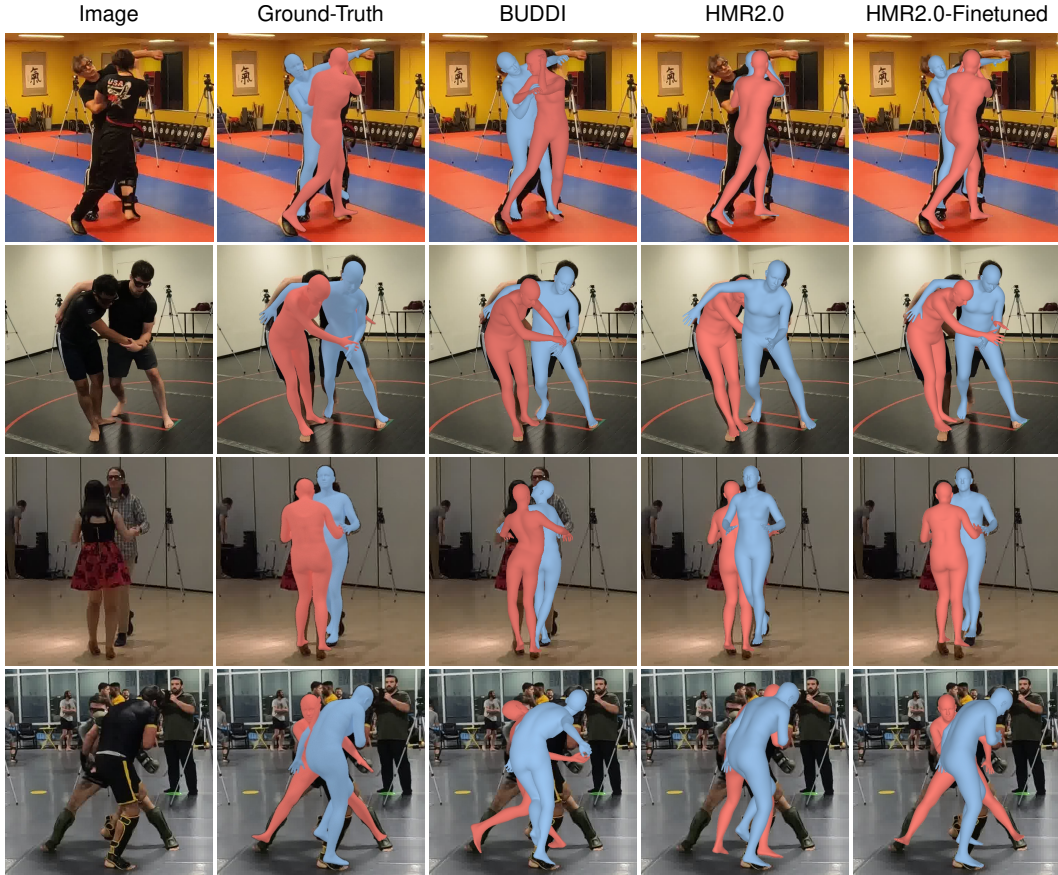


Figure 9: **Qualitative comparison of mesh estimation methods.** We evaluate all methods using ground-truth bounding boxes for fairness. HMR2.0 finetuned on the Harmony4D train set, demonstrates robustness to inter-person occlusion and improved 3D in-contact estimation.

activities in our dataset. We observe that increasing the number of cameras predictably improves performance, as more cameras imply a higher likelihood of a larger inlier set during RANSAC in triangulation. Interestingly, 16 cameras offer a fair trade-off between accuracy and processing speed.

**Interpenetration Loss.** We examine the impact of interpenetration loss on our mesh optimization. We evaluate using the following collision metrics: maximum point-to-surface distance (mP2S) in mm, maximum volumetric IoU (mIoU), and maximum intersection of area (mIoA) in  $m^2$ . Table 3 demonstrates a significant improvement in all collision metrics across sequences. Specifically, on average, mP2S is reduced by 44.7 mm, mIoU is reduced by 0.7%, and mIoA is reduced by  $0.1 m^2$ .

Event	No Loss			Interpenetration Loss		
	mP2S ↓	mIoU ↓	mIoA ↓	mP2S ↓	mIoU ↓	mIoA ↓
Hugging	111.14	1.59	0.24	51.50	0.40	0.07
Wrestling	102.88	0.79	0.16	95.00	0.61	0.10
Dancing	114.91	1.41	0.18	65.60	0.79	0.12
Karate	113.70	0.94	0.16	44.97	0.25	0.06
MMA	122.01	2.26	0.31	83.99	1.43	0.18

Table 3: Adopting the interpenetration loss in mesh optimization significantly improves multi-human collision metrics across activities in the Harmony4D dataset.

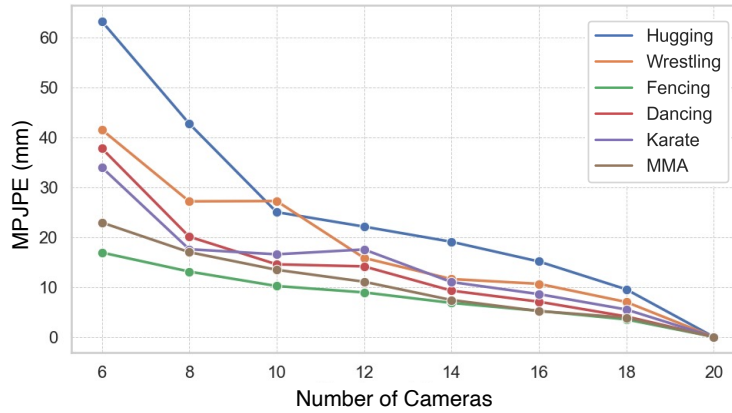


Figure 10: 3D pose triangulation error with varying number of cameras for various interaction activities.

## 5 Conclusion

We propose a novel method to track, segment, and localize 4D body meshes of multiple people interacting in close range with frequent dynamic physical contact under in-the-wild conditions. Our key idea is to use multi-view segmentation-conditioned pose estimation, 3D motion models for forecasting, and collision optimization to obtain precise body model parameters. Using this method, we constructed the diverse Harmony4D dataset with ground-truth annotations for mesh recovery. Emphasis is placed on capturing unchoreographed, dynamic activities such as wrestling, dancing, karate, and MMA in the real world. Our evaluations show that existing state-of-the-art methods fail significantly under the challenging sequences of our dataset, mainly due to the lack of representation of human-human contact interactions in training. Importantly, fine-tuning baselines on our large training set improves mesh estimation performance in severe occlusion and contact conditions.

**Limitations.** We currently trade off the accuracy of 3D pose and shape estimation under contact interactions in favor of capturing in the wild. By adopting an optimization perspective from a dense and mobile camera rig, we enable markerless large-scale capture, complementing high-precision static indoor wired 3D capture systems with limited diversity.

## References

- [1] Antonio Adán, Fernando Molina, Andrés S Vázquez, and Luis Morena. 3d feature tracking using a dynamic structured light system. In *The 2nd Canadian Conference on Computer and Robot Vision (CRV'05)*, pages 168–175. IEEE, 2005.
- [2] Mary B Alatise and Gerhard P Hancke. Pose estimation of a mobile robot based on fusion of imu data and vision data using an extended kalman filter. *Sensors*, 17(10):2164, 2017.
- [3] Fabien Baradel, Matthieu Armando, Salma Galaaoui, Romain Brégier, Philippe Weinzaepfel, Grégory Rogez, and Thomas Lucas. Multi-hmr: Multi-person whole-body human mesh recovery in a single shot. *arXiv preprint arXiv:2402.14654*, 2024.
- [4] Bharat Lal Bhatnagar, Xianghui Xie, Ilya A Petrov, Cristian Sminchisescu, Christian Theobalt, and Gerard Pons-Moll. Behave: Dataset and method for tracking human object interactions. In *Proceedings of the IEEE/CVF Conference on Computer Vision and Pattern Recognition*, pages 15935–15946, 2022.
- [5] Michael J Black, Priyanka Patel, Joachim Tesch, and Jinlong Yang. Bedlam: A synthetic dataset of bodies exhibiting detailed lifelike animated motion. In *Proceedings of the IEEE/CVF Conference on Computer Vision and Pattern Recognition*, pages 8726–8737, 2023.
- [6] Federica Bogo, Angjoo Kanazawa, Christoph Lassner, Peter Gehler, Javier Romero, and Michael J Black. Keep it smpl: Automatic estimation of 3d human pose and shape from a single image. In *European conference on computer vision*, pages 561–578. Springer, 2016.
- [7] Léon Bottou. Stochastic gradient descent tricks. *Neural Networks: Tricks of the Trade: Second Edition*, pages 421–436, 2012.

- [8] Long Chen, Haizhou Ai, Rui Chen, Zijie Zhuang, and Shuang Liu. Cross-view tracking for multi-human 3d pose estimation at over 100 fps. In *Proceedings of the IEEE/CVF conference on computer vision and pattern recognition*, pages 3279–3288, 2020.
- [9] Hongsuk Choi, Gyeongsik Moon, and Kyoung Mu Lee. Pose2mesh: Graph convolutional network for 3d human pose and mesh recovery from a 2d human pose. In *European Conference on Computer Vision*, pages 769–787. Springer, 2020.
- [10] Marius Cordts, Mohamed Omran, Sebastian Ramos, Timo Rehfeld, Markus Enzweiler, Rodrigo Benenson, Uwe Franke, Stefan Roth, and Bernt Schiele. The cityscapes dataset for semantic urban scene understanding. In *Proceedings of the IEEE conference on computer vision and pattern recognition*, pages 3213–3223, 2016.
- [11] Jia Deng, Wei Dong, Richard Socher, Li-Jia Li, Kai Li, and Li Fei-Fei. Imagenet: A large-scale hierarchical image database. In *2009 IEEE conference on computer vision and pattern recognition*, pages 248–255. Ieee, 2009.
- [12] Sai Kumar Dwivedi, Nikos Athanasiou, Muhammed Kocabas, and Michael J Black. Learning to regress bodies from images using differentiable semantic rendering. In *Proceedings of the IEEE/CVF International Conference on Computer Vision*, pages 11250–11259, 2021.
- [13] Monika Eckstein, Ilshat Mamaev, Beate Ditzen, and Uta Sailer. Calming effects of touch in human, animal, and robotic interaction—scientific state-of-the-art and technical advances. *Frontiers in psychiatry*, 11:555058, 2020.
- [14] Zicong Fan, Omid Taheri, Dimitrios Tzionas, Muhammed Kocabas, Manuel Kaufmann, Michael J Black, and Otmar Hilliges. Arctic: A dataset for dexterous bimanual hand-object manipulation. In *Proceedings of the IEEE/CVF Conference on Computer Vision and Pattern Recognition*, pages 12943–12954, 2023.
- [15] Mihai Fieraru, Mihai Zanfir, Elisabeta Oneata, Alin-Ionut Popa, Vlad Olaru, and Cristian Sminchisescu. Three-dimensional reconstruction of human interactions. In *Proceedings of the IEEE/CVF Conference on Computer Vision and Pattern Recognition*, pages 7214–7223, 2020.
- [16] Andreas Geiger, Philip Lenz, Christoph Stiller, and Raquel Urtasun. Vision meets robotics: The kitti dataset. *The International Journal of Robotics Research*, 32(11):1231–1237, 2013.
- [17] Stuart Geman. Statistical methods for tomographic image restoration. *Bull. Internat. Statist. Inst.*, 52:5–21, 1987.
- [18] Shubham Goel, Georgios Pavlakos, Jathushan Rajasegaran, Angjoo Kanazawa, and Jitendra Malik. Humans in 4d: Reconstructing and tracking humans with transformers, 2023.
- [19] Shanyan Guan, Jingwei Xu, Yunbo Wang, Bingbing Ni, and Xiaokang Yang. Bilevel online adaptation for out-of-domain human mesh reconstruction. In *Proceedings of the IEEE/CVF Conference on Computer Vision and Pattern Recognition*, pages 10472–10481, 2021.
- [20] Wen Guo, Xiaoyu Bie, Xavier Alameda-Pineda, and Francesc Moreno-Noguer. Multi-person extreme motion prediction. In *Proceedings of the IEEE/CVF Conference on Computer Vision and Pattern Recognition*, pages 13053–13064, 2022.
- [21] Richard Hartley and Andrew Zisserman. *Multiple view geometry in computer vision*. Cambridge university press, 2003.
- [22] Mohamed Hassan, Vasileios Choutas, Dimitrios Tzionas, and Michael J Black. Resolving 3d human pose ambiguities with 3d scene constraints. In *Proceedings of the IEEE/CVF International Conference on Computer Vision*, pages 2282–2292, 2019.
- [23] Kaiming He, Georgia Gkioxari, Piotr Dollár, and Ross Girshick. Mask r-cnn. In *Proceedings of the IEEE international conference on computer vision*, pages 2961–2969, 2017.
- [24] Matthew J Hertenstein, Dacher Keltner, Betsy App, Brittany A Bulleit, and Ariane R Jaskolka. Touch communicates distinct emotions. *Emotion*, 6(3):528, 2006.

- [25] Derek Hoiem, Santosh K Divvala, and James H Hays. Pascal voc 2008 challenge. *World Literature Today*, 24, 2009.
- [26] Tao Hu, Xinyan Zhu, Wei Guo, Kehua Su, et al. Efficient interaction recognition through positive action representation. *Mathematical Problems in Engineering*, 2013, 2013.
- [27] Chun-Hao P Huang, Hongwei Yi, Markus Höschle, Matvey Safroshkin, Tsvetelina Alexiadis, Senya Polikovsky, Daniel Scharstein, and Michael J Black. Capturing and inferring dense full-body human-scene contact. In *Proceedings of the IEEE/CVF Conference on Computer Vision and Pattern Recognition*, pages 13274–13285, 2022.
- [28] Catalin Ionescu, Dragos Papava, Vlad Olaru, and Cristian Sminchisescu. Human3. 6m: Large scale datasets and predictive methods for 3d human sensing in natural environments. *IEEE transactions on pattern analysis and machine intelligence*, 36(7):1325–1339, 2013.
- [29] Karim Isakov, Egor Burkov, Victor Lempitsky, and Yury Malkov. Learnable triangulation of human pose. In *Proceedings of the IEEE/CVF International Conference on Computer Vision*, pages 7718–7727, 2019.
- [30] Wen Jiang, Nikos Kolotouros, Georgios Pavlakos, Xiaowei Zhou, and Kostas Daniilidis. Coherent reconstruction of multiple humans from a single image. In *Proceedings of the IEEE/CVF Conference on Computer Vision and Pattern Recognition*, pages 5579–5588, 2020.
- [31] Hanbyul Joo, Hao Liu, Lei Tan, Lin Gui, Bart Nabbe, Iain Matthews, Takeo Kanade, Shohei Nobuhara, and Yaser Sheikh. Panoptic studio: A massively multiview system for social motion capture. In *Proceedings of the IEEE international conference on computer vision*, pages 3334–3342, 2015.
- [32] Hanbyul Joo, Tomas Simon, and Yaser Sheikh. Total capture: A 3d deformation model for tracking faces, hands, and bodies. In *Proceedings of the IEEE conference on computer vision and pattern recognition*, pages 8320–8329, 2018.
- [33] Angjoo Kanazawa, Michael J Black, David W Jacobs, and Jitendra Malik. End-to-end recovery of human shape and pose. corr abs/1712.06584 (2017). *arXiv preprint arXiv:1712.06584*, 2017.
- [34] Angjoo Kanazawa, Michael J Black, David W Jacobs, and Jitendra Malik. End-to-end recovery of human shape and pose. In *Proceedings of the IEEE conference on computer vision and pattern recognition*, pages 7122–7131, 2018.
- [35] Dacher Keltner. Hands on research: The science of touch. *Greater Good Magazine*, September, 29, 2010.
- [36] Abdullah Ayub Khan, Asif Ali Laghari, and Shafique Ahmed Awan. Machine learning in computer vision: a review. *EAI Endorsed Transactions on Scalable Information Systems*, 8(32): e4–e4, 2021.
- [37] Rawal Khirodkar, Visesh Chari, Amit Agrawal, and Amrisha Tyagi. Multi-hypothesis pose networks: Rethinking top-down pose estimation. *arXiv preprint arXiv:2101.11223*, 2021.
- [38] Rawal Khirodkar, Shashank Tripathi, and Kris Kitani. Occluded human mesh recovery. In *Proceedings of the IEEE/CVF Conference on Computer Vision and Pattern Recognition*, pages 1715–1725, 2022.
- [39] Rawal Khirodkar, Aayush Bansal, Lingni Ma, Richard Newcombe, Minh Vo, and Kris Kitani. Ego-humans: An ego-centric 3d multi-human benchmark. In *Proceedings of the IEEE/CVF International Conference on Computer Vision*, pages 19807–19819, 2023.
- [40] Alexander Kirillov, Eric Mintun, Nikhila Ravi, Hanzi Mao, Chloe Rolland, Laura Gustafson, Tete Xiao, Spencer Whitehead, Alexander C Berg, Wan-Yen Lo, et al. Segment anything. In *Proceedings of the IEEE/CVF International Conference on Computer Vision*, pages 4015–4026, 2023.
- [41] Muhammed Kocabas, Chun-Hao P. Huang, Otmar Hilliges, and Michael J. Black. PARE: Part attention regressor for 3D human body estimation. In *Proceedings International Conference on Computer Vision (ICCV)*, pages 11127–11137. IEEE, October 2021.

- [42] Muhammed Kocabas, Chun-Hao P Huang, Otmar Hilliges, and Michael J Black. Pare: Part attention regressor for 3d human body estimation. *arXiv preprint arXiv:2104.08527*, 2021.
- [43] Muhammed Kocabas, Chun-Hao P Huang, Joachim Tesch, Lea Müller, Otmar Hilliges, and Michael J Black. Spec: Seeing people in the wild with an estimated camera. In *Proceedings of the IEEE/CVF International Conference on Computer Vision*, pages 11035–11045, 2021.
- [44] Markus Kohler et al. *Using the Kalman filter to track human interactive motion: modelling and initialization of the Kalman filter for translational motion*. Citeseer, 1997.
- [45] Jiefeng Li, Can Wang, Hao Zhu, Yihuan Mao, Hao-Shu Fang, and Cewu Lu. Crowdpose: Efficient crowded scenes pose estimation and a new benchmark. In *Proceedings of the IEEE/CVF Conference on Computer Vision and Pattern Recognition*, pages 10863–10872, 2019.
- [46] Jiefeng Li, Chao Xu, Zhicun Chen, Siyuan Bian, Lixin Yang, and Cewu Lu. Hybrik: A hybrid analytical-neural inverse kinematics solution for 3d human pose and shape estimation. In *Proceedings of the IEEE/CVF Conference on Computer Vision and Pattern Recognition*, pages 3383–3393, 2021.
- [47] Ruilong Li, Shan Yang, David A Ross, and Angjoo Kanazawa. Ai choreographer: Music conditioned 3d dance generation with aist++. In *Proceedings of the IEEE/CVF International Conference on Computer Vision*, pages 13401–13412, 2021.
- [48] Zhihao Li, Jianzhuang Liu, Zhensong Zhang, Songcen Xu, and Youliang Yan. Cliff: Carrying location information in full frames into human pose and shape estimation. *arXiv preprint arXiv:2208.00571*, 2022.
- [49] Kevin Lin, Lijuan Wang, and Zicheng Liu. Mesh graphormer. In *ICCV*, 2021.
- [50] Kevin Lin, Lijuan Wang, and Zicheng Liu. End-to-end human pose and mesh reconstruction with transformers. In *Proceedings of the IEEE/CVF Conference on Computer Vision and Pattern Recognition*, pages 1954–1963, 2021.
- [51] Tsung-Yi Lin, Michael Maire, Serge Belongie, James Hays, Pietro Perona, Deva Ramanan, Piotr Dollár, and C Lawrence Zitnick. Microsoft coco: Common objects in context. In *Computer Vision—ECCV 2014: 13th European Conference, Zurich, Switzerland, September 6–12, 2014, Proceedings, Part V 13*, pages 740–755. Springer, 2014.
- [52] Matthew Loper, Naureen Mahmood, Javier Romero, Gerard Pons-Moll, and Michael J Black. Smpl: A skinned multi-person linear model. *ACM transactions on graphics (TOG)*, 34(6):1–16, 2015.
- [53] Bin Luo and Edwin R Hancock. Iterative procrustes alignment with the em algorithm. *Image and Vision Computing*, 20(5-6):377–396, 2002.
- [54] Zhaoyang Lv, Edward Miller, Jeff Meissner, Luis Pesqueira, Chris Sweeney, Jing Dong, Lingni Ma, Pratik Patel, Pierre Moulon, Kiran Somasundaram, Omkar Parkhi, Yuyang Zou, Nikhil Raina, Steve Saarinen, Yusuf M Mansour, Po-Kang Huang, Zijian Wang, Anton Troynikov, Raul Mur Artal, Daniel DeTone, Daniel Barnes, Elizabeth Argall, Andrey Lobanovskiy, David Jaeyun Kim, Philippe Bouttefroy, Julian Straub, Jakob Julian Engel, Prince Gupta, Mingfei Yan, Renzo De Nardi, and Richard Newcombe. Aria pilot dataset. <https://about.facebook.com/realitylabs/projectaria/datasets>, 2022.
- [55] Naureen Mahmood, Nima Ghorbani, Nikolaus F Troje, Gerard Pons-Moll, and Michael J Black. Amass: Archive of motion capture as surface shapes. In *Proceedings of the IEEE/CVF international conference on computer vision*, pages 5442–5451, 2019.
- [56] Dushyant Mehta, Helge Rhodin, Dan Casas, Pascal Fua, Oleksandr Sotnychenko, Weipeng Xu, and Christian Theobalt. Monocular 3d human pose estimation in the wild using improved cnn supervision. In *2017 international conference on 3D vision (3DV)*, pages 506–516. IEEE, 2017.
- [57] Dushyant Mehta, Oleksandr Sotnychenko, Franziska Mueller, Weipeng Xu, Srinath Sridhar, Gerard Pons-Moll, and Christian Theobalt. Single-shot multi-person 3d pose estimation from monocular rgb. In *2018 International Conference on 3D Vision (3DV)*, pages 120–130. IEEE, 2018.

- [58] Lea Müller, Vickie Ye, Georgios Pavlakos, Michael Black, and Angjoo Kanazawa. Generative proxemics: A prior for 3d social interaction from images. *arXiv preprint arXiv:2306.09337*, 2023.
- [59] Dinesh K Pai, Austin Rothwell, Pearson Wyder-Hodge, Alistair Wick, Ye Fan, Egor Larionov, Darcy Harrison, Debanga Raj Neog, and Cole Shing. The human touch: Measuring contact with real human soft tissues. *ACM Transactions on Graphics (TOG)*, 37(4):1–12, 2018.
- [60] Priyanka Patel, Chun-Hao P Huang, Joachim Tesch, David T Hoffmann, Shashank Tripathi, and Michael J Black. Agora: Avatars in geography optimized for regression analysis. In *Proceedings of the IEEE/CVF Conference on Computer Vision and Pattern Recognition*, pages 13468–13478, 2021.
- [61] Georgios Pavlakos, Vasileios Choutas, Nima Ghorbani, Timo Bolkart, Ahmed AA Osman, Dimitrios Tzionas, and Michael J Black. Expressive body capture: 3d hands, face, and body from a single image. In *Proceedings of the IEEE/CVF conference on computer vision and pattern recognition*, pages 10975–10985, 2019.
- [62] Georgios Pavlakos, Jitendra Malik, and Angjoo Kanazawa. Human mesh recovery from multiple shots. In *Proceedings of the IEEE/CVF Conference on Computer Vision and Pattern Recognition*, pages 1485–1495, 2022.
- [63] Leonid Pishchulin, Stefanie Wuhrer, Thomas Helten, Christian Theobalt, and Bernt Schiele. Building statistical shape spaces for 3d human modeling. *Pattern Recognition*, 2017.
- [64] Pirkko Routasalo. Physical touch in nursing studies: a literature review. *Journal of Advanced Nursing*, 30(4):843–850, 1999.
- [65] Johannes L Schonberger and Jan-Michael Frahm. Structure-from-motion revisited. In *Proceedings of the IEEE conference on computer vision and pattern recognition*, pages 4104–4113, 2016.
- [66] Soyong Shin, Juyong Kim, Eni Halilaj, and Michael J Black. Wham: Reconstructing world-grounded humans with accurate 3d motion. *arXiv preprint arXiv:2312.07531*, 2023.
- [67] Leonid Sigal, Alexandru O Balan, and Michael J Black. Humaneva: Synchronized video and motion capture dataset and baseline algorithm for evaluation of articulated human motion. *International journal of computer vision*, 87(1-2):4, 2010.
- [68] Ke Sun, Bin Xiao, Dong Liu, and Jingdong Wang. Deep high-resolution representation learning for human pose estimation. In *Proceedings of the IEEE/CVF Conference on Computer Vision and Pattern Recognition*, pages 5693–5703, 2019.
- [69] Yu Sun, Qian Bao, Wu Liu, Yili Fu, Michael J Black, and Tao Mei. Monocular, one-stage, regression of multiple 3d people. In *Proceedings of the IEEE/CVF international conference on computer vision*, pages 11179–11188, 2021.
- [70] Yu Sun, Wu Liu, Qian Bao, Yili Fu, Tao Mei, and Michael J Black. Putting people in their place: Monocular regression of 3d people in depth. In *Proceedings of the IEEE/CVF Conference on Computer Vision and Pattern Recognition*, pages 13243–13252, 2022.
- [71] Omid Taheri, Nima Ghorbani, Michael J Black, and Dimitrios Tzionas. Grab: A dataset of whole-body human grasping of objects. In *Computer Vision–ECCV 2020: 16th European Conference, Glasgow, UK, August 23–28, 2020, Proceedings, Part IV 16*, pages 581–600. Springer, 2020.
- [72] Shashank Tripathi, Agniv Chatterjee, Jean-Claude Passy, Hongwei Yi, Dimitrios Tzionas, and Michael J Black. Deco: Dense estimation of 3d human-scene contact in the wild. In *Proceedings of the IEEE/CVF International Conference on Computer Vision*, pages 8001–8013, 2023.
- [73] Jan BF Van Erp and Alexander Toet. Social touch in human–computer interaction. *Frontiers in digital humanities*, 2:2, 2015.

- [74] Coert Van Gemeren, Ronald Poppe, and Remco C Veltkamp. Spatio-temporal detection of fine-grained dyadic human interactions. In *Human Behavior Understanding: 7th International Workshop, HBU 2016, Amsterdam, The Netherlands, October 16, 2016, Proceedings 7*, pages 116–133. Springer, 2016.
- [75] Timo von Marcard, Roberto Henschel, Michael J Black, Bodo Rosenhahn, and Gerard Pons-Moll. Recovering accurate 3d human pose in the wild using imus and a moving camera. In *Proceedings of the European Conference on Computer Vision (ECCV)*, pages 601–617, 2018.
- [76] Han Xiao, Kashif Rasul, and Roland Vollgraf. Fashion-mnist: a novel image dataset for benchmarking machine learning algorithms. *arXiv preprint arXiv:1708.07747*, 2017.
- [77] Sirui Xu, Zhengyuan Li, Yu-Xiong Wang, and Liang-Yan Gui. Interdiff: Generating 3d human-object interactions with physics-informed diffusion. In *Proceedings of the IEEE/CVF International Conference on Computer Vision*, pages 14928–14940, 2023.
- [78] Yufei Xu, Jing Zhang, Qiming Zhang, and Dacheng Tao. Vitpose: Simple vision transformer baselines for human pose estimation. *Advances in Neural Information Processing Systems*, 35: 38571–38584, 2022.
- [79] Hongwei Yi, Chun-Hao P. Huang, Dimitrios Tzionas, Muhammed Kocabas, Mohamed Hassan, Siyu Tang, Justus Thies, and Michael J. Black. Human-aware object placement for visual environment reconstruction. In *Computer Vision and Pattern Recognition (CVPR)*, June 2022.
- [80] Yifei Yin, Chen Guo, Manuel Kaufmann, Juan Zarate, Jie Song, and Otmar Hilliges. Hi4d: 4d instance segmentation of close human interaction. In *Computer Vision and Pattern Recognition (CVPR)*, 2023.
- [81] Zhixuan Yu, Jae Shin Yoon, In Kyu Lee, Prashanth Venkatesh, Jaesik Park, Jihun Yu, and Hyun Soo Park. Humbi: A large multiview dataset of human body expressions. In *Proceedings of the IEEE/CVF Conference on Computer Vision and Pattern Recognition*, pages 2990–3000, 2020.
- [82] Ailing Zeng, Xiao Sun, Fuyang Huang, Minhao Liu, Qiang Xu, and Stephen Lin. Srnet: Improving generalization in 3d human pose estimation with a split-and-recombine approach. In *European Conference on Computer Vision*, pages 507–523. Springer, 2020.
- [83] Hongwen Zhang, Yating Tian, Xinchu Zhou, Wanli Ouyang, Yebin Liu, Limin Wang, and Zhenan Sun. Pymaf: 3d human pose and shape regression with pyramidal mesh alignment feedback loop. In *Proceedings of the IEEE/CVF International Conference on Computer Vision*, pages 11446–11456, 2021.
- [84] Song-Hai Zhang, Ruilong Li, Xin Dong, Paul Rosin, Zixi Cai, Xi Han, Dingcheng Yang, Haozhi Huang, and Shi-Min Hu. Pose2seg: Detection free human instance segmentation. In *Proceedings of the IEEE/CVF Conference on Computer Vision and Pattern Recognition*, pages 889–898, 2019.
- [85] Xiang Zhang, Stephan Frönz, and Nassir Navab. Visual marker detection and decoding in ar systems: A comparative study. In *Proceedings. International Symposium on Mixed and Augmented Reality*, pages 97–106. IEEE, 2002.
- [86] Yifu Zhang, Peize Sun, Yi Jiang, Dongdong Yu, Fucheng Weng, Zehuan Yuan, Ping Luo, Wenyu Liu, and Xinggang Wang. Bytetrack: Multi-object tracking by associating every detection box. In *European Conference on Computer Vision*, pages 1–21. Springer, 2022.
- [87] Yang Zheng, Ruizhi Shao, Yuxiang Zhang, Tao Yu, Zerong Zheng, Qionghai Dai, and Yebin Liu. Deepmulticap: Performance capture of multiple characters using sparse multiview cameras. In *Proceedings of the IEEE/CVF International Conference on Computer Vision*, pages 6239–6249, 2021.
- [88] Yi Zhou, Connelly Barnes, Jingwan Lu, Jimei Yang, and Hao Li. On the continuity of rotation representations in neural networks. In *Proceedings of the IEEE/CVF Conference on Computer Vision and Pattern Recognition*, pages 5745–5753, 2019.